Adherens junction remodeling by the Notch pathway in Drosophila melanogaster oogenesis.

Muriel Grammont

The Journal of Cell Biology 177, 1 (2007) 139-50

Adherens junction remodelling by the Notch pathway in *Drosophila melanogaster* oogenesis

Muriel Grammont

Inserm, U384; Univ Clermont 1, UFR Médecine, Clermont-Ferrand, F-63001 France.

Phone: 33 4 73 17 83 80

Fax: 33 4 73 27 61 32

Email: muriel.grammont@inserm.u-clermont1.fr

Short Title: Notch and follicular cell morphogenesis

Key Words: *fringe*, *Notch*, adherens junction, follicular cell

Abstract

Identifying genes involved in the control of adherens junction (AJ) remodelling is essential to understanding epithelial morphogenesis. During follicular epithelium development in *Drosophila*, the main body follicular cells (MBFC) are displaced towards the oocyte, and become columnar. Concomitantly, the stretched cells (StC) become squamous and flatten around the nurse cells. By monitoring the expression of E Cadherin and Armadillo, I have discovered that the rate of AJ disassembly between the StC is affected in follicles with somatic clones mutant for *fringe* or *Delta* and *Serrate*. This results in abnormal StC flattening and delayed MBFC displacement. Additionally, the accumulation of the Myosin II heavy chain, Zipper, is delayed at the AJ that require disassembly. Together, my results demonstrate that the N pathway controls AJ remodelling between the StC, and that this role is crucial for the timing of MBFC displacement and StC flattening. This provides new evidence that Notch, besides playing a key role in cell differentiation, also controls cell morphogenesis.

Introduction

Epithelial cell morphogenesis is a key step in the formation and the development of multicellular organisms. Morphogenetic processes involving cell shape change or cell displacement inside an epithelial sheet depend on the flexibility of the cohesiveness between epithelial cells, which is ensured by several adhesion systems, such as the adherens junctions. Elucidating the regulation of the expression of molecules involved in cellular adhesion is thus crucial to increasing our knowledge of epithelial cell morphogenesis. The somatic follicular cells of *Drosophila* ovarian follicles provide a simple system for studying epithelial morphogenesis. Initially, these cells have a cuboidal shape and form a monolayer around each 16-cell germline cyst. Throughout oogenesis, they progressively differentiate into distinct populations that adopt a squamous or columnar shape and undergo various morphogenetic movements. Thus, studying cell morphogenesis of the follicular epithelium should further our understanding of how cell shape change and cell displacement proceed in an epithelial sheet.

When a follicle leaves the germarium (stage 1), it consists of a germ cyst of 16 cells (1 oocyte and 15 nurse cells (NC)) surrounded by a monolayer of follicular cells (Fig. 1) (Spradling, 1993). Three different subpopulations of somatic cells can be identified: the polar cells, the stalk cells and the follicular cells (Fig. 1A). Two pairs of polar cells are present at each extremity of the follicle, while the interfollicular cells are organized into a stalk of 4 to 6 cells that intercalate between adjacent follicles. These two populations play a critical role in follicle formation (Grammont and Irvine, 2001; Lopez-

Schier and St Johnston, 2001; Torres et al., 2003). The differentiation of the follicular epithelium starts with the specification of the terminal follicular cells versus the main body follicular cells (MBFC) (Gonzalez-Reyes et al., 1995; Roth et al., 1995). At the anterior pole, the terminal cells give rise to the border cells, the stretched cells (StC) and the centripetal cells (Fig. 1A). These three populations cannot be recognized prior to stage 9 or 10, when specific markers or genes are expressed and several morphogenetic features become apparent (Dobens and Raftery, 2000; Horne-Badovinac and Bilder, 2005; Spradling, 1993). Of relevance to this work are the morphogenetic processes that concern the MBFC and the StC: at stage 9, the MBFC displace towards the oocyte and take on a columnar shape when they make contact with it, while the StC flatten around the NC to maintain a continuous epithelium. This flattening starts from the most anterior cells and extends progressively to the cells located more posteriorly. This process can be monitored by the expression of the MA33 and *decapentaplegic* (*dpp*) enhancer trap lines and of the Eyes absent protein (Eya) (See materials and methods). At the end of the process of StC flattening, most of the nuclei of the fifty or so stretched cells are positioned in the interstitial gaps between the NC (Fig. 1B) (Spradling, 1993). The rearrangement of the MBFC into columnar cells, their displacement towards the oocyte and the flattening of the StC are morphogenetic processes that are poorly understood and the genes involved almost entirely unknown.

The Notch signalling pathway is required at several stages of oogenesis. First, the Notch (N) receptor is required for polar cell

differentiation in the germarium. This entails the germline production of the ligand Delta (Dl) and the specific expression of the Notch modulator Fringe (Fng) in the polar cell precursors (Grammont and Irvine, 2001; Lopez-Schier and St Johnston, 2001; Torres et al., 2003). Second, the Notch signalling pathway is required to induce a transition from mitotic cycle to endocycle in the follicular cells at stage 6 of oogenesis. This role is also dependent on the germline production of Dl, but is *fng*-independent (Deng et al., 2001). Third, stage 10 follicles mutant for *N* display defects in the differentiation of the border, stretched and centripetal cells as well as abnormal migration (Dobens et al., 2005; Gonzalez-Reyes and St Johnston, 1998; Keller Larkin et al., 1999; Zhao et al., 2000). Although the first two requirements of *N* have been analysed in detail, the third is poorly defined, since it has only been demonstrated using a *N* thermo-sensitive allele. Thus, the precise role of N in the differentiation of the border, stretched and centripetal cells and in their morphogenesis remains an unresolved question.

Here I have taken a different approach to address this question by analysing the role of *fng* during StC flattening and MBFC displacement, as its expression pattern from stage 7 to stage 10A suggested that it could be involved. Indeed, during these stages, *fng* mRNA is present in all the follicular cells, except the outer border cells (Grammont and Irvine, 2001; Zhao et al., 2000). Somatic mutant clones for a *fng* null allele (fng^{13}) have been generated and analysis of the phenotypes induced by the mutant clones leads to the conclusion that the N pathway functions in a *fng*-dependant manner to control adherens junction remodelling between the StC and that

this activity is essential for proper StC flattening and for the timing of MBFC displacement.

Results

fringe is required in the StC and the anterior MBFC to control StC number and the timing of MBFC displacement

Since *fng* is required for the differentiation of polar cells, which in turn promote terminal cell differentiation (Beccari et al., 2002; Grammont and Irvine, 2002; Silver and Montell, 2001; Xi et al., 2003), only follicles with somatic fng^{13} clones that do not include the anterior and posterior polar cells were analysed. Only the role of *fng* in the MBFC displacement and StC flattening will be analysed in detail here. In the phenotypic description, references to the MBFC include the cells destined to become centripetal cells since the two cell types are indistinguishable until stage 10 (Fig. 1A). When fng^{13} clones encompass some StC and some MBFC, an excess of cells is observed over the NC in follicles at stage 10A or older (75%, n=60). As described in the next two paragraphs, these supernumerary cells are either MBFC or StC.

In stage 10A follicles, many of the supernumerary cells appear in clusters (Fig. 2A). These clusters present three traits. First, they display a cell density more characteristic of the MBFC population than of the StC population. Second, they are always immediately adjacent to the MBFC population. Third, most of their component cells do not express MA33 or Eya, except the ones that are at the anterior border of the cluster (Fig. 2B), indicating that the majority of these cells do not have a stretched fate. Together, these data suggest that most of the supernumerary cells within these clusters are MBFC that did not fully complete their displacement. In agreement with that, these clusters are never observed over the NC

at later stages, indicating that they do eventually surround the oocyte (Fig. 2C). Thus, these observations show that *fng* is required in the StC and in the MBFC to allow the posterior displacement of the MBFC to be fully completed by the end of stage 9. However, since this displacement does still occur, other mechanisms must act in parallel to *fng* to control it.

In stage 10B follicles, supernumerary cells, although no longer arranged in clusters, are still observed over the NC when a large clone encompasses some MBFC and some StC (80%, n=25). These supernumerary cells express every StC marker such as MA33 (Fig. 2D), Eya (Fig. 5A), *dpp-lacZ* and the Dpp pathway read-out *Dad-lacZ*, the latter also being expressed in the StC during their flattening (see Materials and methods). Thus, all the supernumerary cells that are observed over the NC in stage 10B follicles have a StC fate. As a consequence, in such follicles, the number of StC increases from about 50 to between 70 and 110 cells (Fig. 2D). These extra StC could either have arisen from extra divisions of the fng^{13} cells or from MBFC that did not get displaced and instead adopted a stretched fate. If these were abnormally proliferating follicular cells, a much higher density of cells would be expected in the part of the mutant clone overlying the NC, as has been shown for mutant alleles of genes required to stop follicular cell mitotic division (Deng et al., 2001). Moreover, no expression of Cyclin B and Phospho-Histone3 has been detected in *fng* mutant clones after stage 6 of oogenesis (Deng et al., 2001; Grammont, unpublished data). Thus, these cells are most likely MBFC that did not reached the oocyte and differentiated as StC. In conclusion, the supernumerary cells

observed above the NC at stages 10A and 10B derive from an abnormal displacement of the MBFC.

The penetrance and the expressivity of these phenotypes vary based on the type and the number of cells that are mutant. The penetrance is higher when the clones encompass both MBFC and StC than when they encompass only one of those cell types, showing that *fng* is required in both the StC and the MBFC. Nevertheless, when the clones encompass just MBFC, only clones in the anterior part of the MBFC population induce delayed displacement (Fig. 2E), while follicles with a large lateral and/or posterior clone do not (Grammont, unpublished data). This indicates that the requirement of *fng* is different within the MBFC population, with a higher requirement in the anterior cells in contact with the StC. On the other hand, the displacement of the MBFC is more delayed in regions where most of the StC are mutant than in regions where most of the StC are wild type (WT), indicating that the StC play an essential role in MBFC displacement (Fig. 2F). Finally, MBFC delays are rarely (6%, n=30) observed in small clones (less than 10 cells) (Grammont, unpublished data), suggesting that the presence of WT cells around the mutant cells prevents it. Equally, some WT MBFC can be delayed when they are in the immediate proximity of a large clone (Fig. 2B, 5A). This suggests that the process of displacement for one MBFC depends on the ability of its neighbouring cells to be displaced, such that the displacement of the MBFC occurs in a coordinated manner all around the follicle, and not in a cell autonomous manner. In conclusion, *fng* is required in the StC and the anterior MBFC to direct StC number and to control the timing of MBFC displacement.

fringe is not required for StC differentiation

It has been proposed that the displacement of the MBFC towards the oocyte is due to cell shape changes of the most posterior cells from cuboidal to columnar, with this change in form forcing their neighbouring anterior cells to move posteriorly (Horne-Badovinac and Bilder, 2005; Spradling, 1993). Because no MBFC displacement delay is observed in *fng*^{13} clones encompassing only posterior cells and because no defect in cell shape change has been detected in *fng*^{13} posterior cells, *fng* is not required to generate the force created by the posterior cells (henceforth referred to as the 'pulling force') (Grammont, unpublished data). In WT follicles, the MBFC displacement probably stops when the StC are unable to expand any further without compromising the integrity of the epithelium, implying that this displacement also depends on the ability of the cells to respond to the pulling force, for example by flattening. It is then likely that *fng* is involved in this response, since a delayed MBFC displacement is observed in most follicles with a *fng*^{13} clone encompassing StC and anterior MBFC.

In fact, defective StC flattening and delayed MBFC displacement could arise from a physical inability to undergo morphogenetic processes or from an abnormal StC differentiation (Xi et al., 2003). Accordingly, an analysis of the expression of all known StC fate markers - the Eya protein and the *MA33* and *dpp-lacZ* and *Dad-lacZ* enhancer-traps - has been undertaken in stage 9 follicles containing an anterior clone on one side of the follicle. This provides an internal reference, such that marker expression in mutant cells can be compared to WT cells located at the same anterior-posterior (A/P)

position. No noticeable difference in the expression of any of the markers was observed between WT and *fng* mutant StC (Fig. 3A, 3B, 3C), indicating that the differentiation of the *fng* mutant StC is not delayed in comparison with the WT cells. Moreover, although the role of the Dpp pathway in StC fate determination is unknown, the correct expression of the *Dad-lacZ* enhancer trap in fng^{13} StC rules out the hypothesis that this pathway is not active in these cells (Fig. 3B). In conclusion, no significant alteration of StC identity is observed in *fng* mutant follicles.

The Notch pathway controls the dynamics of AJ remodelling

Since the delay in MBFC displacement in fng^{13} clones is not due to a delay in StC differentiation, it leaves open two possibilities: either that *fng* mutant StC are unable to flatten properly and/or that *fng* mutant MBFC cannot move posteriorly properly. One possible underlying cause that could explain both possibilities is a physical inability for the cells to change their shapes and/or to be displaced. Epithelial cell shape change and movement depends on adherens junction (AJ) remodelling. A detailed analysis of AJ remodelling was first carried out in WT stage 9 follicles because this is as of yet uncharacterised. Since the StC undergo the greatest cell shape changes within a follicle, it is reasonable to expect that any mutation that causes defects in cell shape changes by modifying the properties of AJ may manifest more dramatically in the StC than in any other cell types.

Therefore, to simplify the study of the role of *fng*, I have chosen to focus on the AJ and their dynamics between the StC, by

monitoring the expression of E Cadherin (ECad) (Fig. 4) and the β-catenin protein, Armadillo (Supplemental data S1). The following observations have been obtained from analysis of an mean of 15 follicles of each stage. Throughout stage 9, a colocalisation between the two proteins is observed. In early stage 9 of oogenesis, a strong ECad expression is detected in all follicular cells, except the posterior cells. This expression displays the hexagonal shape of the follicular cells, indicating that AJ are present all around each cell close to their apical side (Fig. 4A). Due to the geometry of the cells, some AJ mediate contact between two cells, whilst others between three (Fig. 4A). The orientations of the two-cell junctions are essentially either perpendicular or parallel to the A/P axis. During the process of flattening (mid stage 9), no ECad expression is detected at the three-cell junctions that mediate contact between the flattened cells and the flattening cells (Fig. 4B). In contrast, ECad is still present at the three-cell junctions that mediate contact between the flattening cells and the unflattened cells. Additionally, only a few spots of ECad are observed in the perpendicularly-oriented two-cell junctions between the flattened cells and the flattening cells whereas a strong ECad expression is still observed in those between the flattening cells and the unflattened cells (Fig. 4B). Distinct patterns are thus observed depending on the degree of flattening of the cells. In late stage 9, most of the AJ are no longer visible except for the ones that are parallel to the A/P axis (Fig. 4C). At stage 10A, these junctions are barely visible, but ECad starts to be accumulated very strongly in the part of the StC located in the intersticial gaps between NC. ECad is also detected weakly in the part of the StC overlying the NC (Fig. 4D).

At stage 10B, the AJ parallel to the A/P axis are no longer detected, but the ECad expression in the part of the StC overlying the NC increase, which permits the detection of the shape of the StC. This reveals that most of the StC are more elongated along the A/P axis than along the dorsal-ventral axis (Fig. 4E). Identical results for StC shape were also obtained by assaying α-Tubulin expression (Fig. 4F).

To summarise, ECad expression strongly increases just before the MBFC displacement and the StC flattening. In the StC undergoing flattening, the three-cell junctions disassemble first, promptly followed by all the two-cell junctions perpendicular to the A/P orientation and then the two-cell junctions parallel to the A/P orientation. This highly dynamic expression permits the monitoring of the flattening of the StC and of their shape once the flattening is completed. This ECad expression pattern shows that the process of flattening is coordinated all around the follicle, since it starts from the anteriormost row of cells and progresses posteriorly row by row. Finally, the dynamic of this pattern suggests that the order of disassembly of the AJ during stage 9 dictates the direction of cell flattening, allowing the cells to spread and adopt an elongated shape along the A/P axis.

Next I compared ECad expression patterns in *fng*^{13} mutant StC to control WT StC located at the same A/P position within the follicle. At late stage 9, the three-cell junctions between WT cells are disassembled, whereas they are still intact in regions where most of the StC are mutant (77%, n=18) (Fig. 5A, arrows). The StC immediately posterior to these latter mutant StC, whether themselves WT or mutant (Fig. 5A, large arrow and arrowhead), display ECad

staining on all their edges, indicating that the process of AJ remodelling has not yet started in these cells. Finally, an abnormally high number of StC, as well as a delay in the MBFC displacement, are observed in the mutant region (77%, n=18). Similar results are obtained by monitoring the expression of Armadillo (75%, n=12) (Supplemental data S1).

Together, these observations show that *fng* is required for the AJ dynamics to occur properly during the StC flattening and, thus, that the MBFC displacement delays and the abnormally high number of StC observed in *fng* mutant follicles derive from a physical inability of the StC to flatten. ECad expression patterns still differ between mutant and WT regions in a stage 10A fng^{13} follicle (Supplemental data S2) but in late stage 10B follicles, the ECad expression pattern is almost identical between mutant and WT regions indicating that AJ remodelling is delayed, but not blocked, in fng^{13} clones (Grammont, unpublished data). In these follicles, when the majority of the StC are mutant, there are twice as many StC as in a WT follicle (Fig. 5B). Since the overall size of the NC compartment in follicles with many mutant StC is not substantially different than in WT, each StC likely covers less surface area than a WT (Compare 5B with 3F). Indeed, the mean surface area of StC in a WT follicle is 1526 ± 301 μm^2 (n=30), whereas the mean surface area of a StC in a follicle with a large fng^{13} clone is 804 ± 261μm^2 (n=83; $p< 0.0001$). This shows that StC in *fng* mutant follicles flatten less than StC in WT follicles. In addition, no accumulation of ECad is observed in the part of the StC that are usually squeezed into the interstitial gaps between the NC, presumably because the StC are less flattened and their nuclei no

longer forced into these gaps. In contrast, a higher level of ECad is detected in the part of the StC overlying the NC (Compare Fig. 5B with 4E). This brighter ECad signal could derive from a higher expression level, but more likely reflects the fact that because the cells are smaller, their apical surface is reduced and ECad molecules are thus more concentrated. Staining for α-tubulin yields identical results (Fig. 5B', 5B''). In conclusion, *fng* is required for the proper flattening of the StC, which in turn controls the minimal number of cells that will adopt this fate.

In order to address whether this role of *fng* is linked to an activity of the N pathway, I conducted a similar analysis with null alleles of *Dl* (Dl^{rev10}) and *Ser* (Ser^{RX106}). This analysis shows that in stage 9 follicles with anterior clones doubly mutant for *Dl* and *Ser*, most of the three-cell junctions are still present in the mutant region, but disassembled in the WT region (91%, n=23) (Fig. 5C). Furthermore, an increased density of StC and a delayed MBFC displacement are observed in the mutant region (Fig. 5C). No defects have been observed for single $Ser^{rev2-11}$ clones (n=8) whereas single Dl^{rev10} clones yielded similar defects with a weaker expressivity to the double *Dl Ser* mutant clones (87%, n=15) (Grammont, unpublished data). In addition, as described for fng^{13} follicles, the appearance of StC markers occurs properly in the *Dl Ser* mutant StC (Grammont, unpublished data). Together, these data demonstrate that, while the Notch pathway appears not to effect StC identity, it does have a *fng*-dependant role in remodelling their AJ, with *Dl* playing an essential role in the soma and *Ser* having an overlapping function.

A detailed analysis of the expression pattern of Notch and Delta during stage 9 reveals that these two proteins are strongly expressed in the flattened and in the flattening StC. In particular, a strong accumulation of N is detected at the disassembling three-cell junctions, suggesting that this expression corresponds to the role of N described here (Fig. 5D,E). Similarly, analyses of the expression patterns of some reporters for N activation show that they are more strongly expressed in the flattened and flattening StC than in the MBFC (Supplemental data S3). Thus the expression patterns of these markers indicate that the N pathway is transcriptionally active in the StC at stage 9. As a direct involvement of the canonical Notch pathway cannot be analysed (due to its requirement at earlier steps of oogenesis), I tested the effects of overexpressing Hairless (H), a repressor of N transcriptional activity, using a *hs-H* construct. In all stage 9 follicles overexpressing H (n=28), abnormal AJ remodelling is observed. In contrast to WT follicles, no AJ disassembly is detected between StC in early-mid stage 9 follicles overexpressing H (Compare Fig. 4B with Fig. 5F). Rather, this disassembly commences only in mid-late stage 9 follicles, after several rows of StC have differentiated (Fig. 5G - Supplemental data S3E). This indicates that the transcriptional activity of Notch plays a crucial role in controlling the dynamics of AJ disassembly between StC at stage 9 of oogenesis.

Follicles expressing a constitutively activated form of Notch (Nact) were then analysed. Surprisingly, the overexpression of Nact in some stretched cells leads to an autonomous abnormal flattening of stretched cells and a delay in AJ remodelling (72%, n=20)

(Supplemental data S3). The shape of Nact-expressing cells remains cuboidal longer than the cells undergoing flattening that are located at the same position along the A/P axis (Fig. S3F). In parallel, the AJ remodelling is delayed in the Nact-expressing region in comparison to the WT region (Fig. S3G). This indicates that some N target genes are involved in the AJ remodelling. One could suggest that the loss or the gain of activity of the N pathway affects the expression of different target genes, or that the timing of N activation has to be controlled very precisely to allow proper AJ remodelling.

The Notch pathway controls the localisation of Myosin II

The chronology of AJ disassembly is essential for the StC flattening and the timing of the MBFC displacement. This chronology likely depends on local effectors at the cell junctions undergoing disruption. The myosin II heavy chain and regulatory light chain, encoded by the *zipper* (*zip*) and the *spaghetti squash* (*sqh*) genes respectively, are two effectors that have been shown to remodel cell junctions in a polarized manner (Bertet et al., 2004). To determine whether these two proteins are involved in junction disassembly during StC flattening, their expression patterns were determined in stage 9 follicles. A detailed analysis during stage 9 shows that Zipper is more strongly accumulated in some specific spots, which correspond to disassembling AJ. Indeed, depending on the degree of the flattening of the StC, Zip can be strongly accumulated along a lateral line that separates the flattened cells from the ones that are flattening (Fig. 6A). Some parts of this line of expression correspond to the edges of the StC that are oriented perpendicular to the A/P

axis. Anterior to this line, Zip is accumulated in StC, both in the vicinity of their nuclei, as well as along those edges that are parallel to the A/P axis. In some follicles, this line is not detected but instead, a strong accumulation is detected at the disassembling three-cell junctions that are between the row of flattening StC and the row of unflattened cells (Fig. 6B). A similar pattern of expression is observed with a Sqh-GFP fusion protein (Fig. 6C). Together, these observations suggest that these are good candidate proteins for the control of the chronology of AJ remodelling during StC flattening.

To confirm this, Zip expression has been investigated in *Dl Ser* double mutant follicles. In such follicles, when the lateral line of Zip accumulation is observed in WT regions, it appears to be interrupted in regions containing mutant cells (Fig. 6D). Moreover, at the A/P position where Zip is accumulated at the disassembling three-cell junctions in WT regions, no accumulation is detected in mutant regions (Fig. 6E). Such accumulations are instead detected at disassembling three-cell junctions located more anteriorly. Hence, the delay in the AJ disassembly observed in Dl^{rev10} Ser^{RX106} cells is coincident with the delay in the appearance of Zip accumulation at disassembling junctions. A similar delay is observed in fng^{13} cells (Grammont, unpublished data). Thus, the defects in StC flattening and MBFC displacement delay may be due to a lack of polarization of Zipper during cell junction disassembly.

E Cadherin and Myosin II are required for StC flattening

As an impaired N pathway results in abnormal delay in AJ remodelling and modification of Zipper expression pattern during StC

flattening, it suggests a role for *shg*, *zip* and *sqh* during this process. In order to test this, somatic mutant clones for a *shg* null allele (shg^{R69}) and for a *sqh* hypomorphic allele (sqh^{1}) were induced. Stage 9 follicles with *shg* mutant clones display a higher density of flattening StC in the mutant region than in WT (n=12) (Fig. 7A, 7A', 7A''). At stage 10, a delay in MBFC displacement is also detected in the mutant region (n=10) (Fig. 7B). Thus, as observed in follicles with *fng* and *Dl*/*Ser* mutant clones, the ability of the StC to flatten and the timing of MBFC displacement are impaired in *shg* mutant follicles. One might expect that the absence of *shg* would result in the loss of AJ and that StC flattening would occur faster and/or without any constraint. In light of this, the data from the *shg* clones could suggest that the cells are still adhesive. As another adhesion molecule, N Cadherin (NCad), can also be a component of AJ, its expression was investigated in such clones. In WT follicles, NCad is strongly expressed in all follicular cells from stage 1 to stage 6 (Fig. 7C). Its expression decreases during stage 7 and 8 to become almost undetectable at stage 9, with a weak expression in the follicular cells that surround the oocyte and in the StC (Fig. 7D). In stage 7-9 follicles with *shg* mutant clones, a strong NCad expression is detected in the mutant cells. This over-expression is cell-autonomous in stage 7 follicles (n=11), but is restricted to the anterior part of the clones in stage 8 (n=9) and stage 9 follicles (75%, n=20) (Fig. 7A''', 7A'''', Supplemental data S4). This over-expression of NCad is no longer detected at stage 10A (n=25) (Grammont, unpublished data). Thus, the absence of ECad is compensated by the up-regulation of NCad from stage 7 to stage 10 and leads to delayed StC flattening

and MBFC displacement, indicating that the levels of ECad and NCad expression during mid oogenesis are interrelated and that the regulation of ECad expression is an important key for StC flattening.

The requirement of Myosin II cannot be tested directly by using null alleles of *zip* or *sqh*, as mutant cells will be unable to divide. Thus a hypomorphic allele of *sqh* was used and only small clones can be analysed. In stage 9 follicles, the *sqh* mutant StC undergoing flattening present an abnormal pattern of ECad. The AJ are not remodelled according to the pattern described for WT cells (Fig. 7E). The elongation of the mutant cells do not appear to occur mainly along the A/P axis, but is more randomly oriented. In addition, the AJ parallel to the A/P axis between cells that have already flattened, are no longer visible in the mutant region when compared to the WT region. This indicates that the activity of the regulatory light chain of the Myosin II is required to control the dynamic of AJ remodelling and proper StC flattening.

Discussion

Three important morphogenetic events occur in the follicular tissues at stage 9 of oogenesis: border cell migration, StC flattening and MBFC displacement. My results have advanced the understanding of StC flattening and MBFC displacement in two crucial ways. First, they demonstrate that the rate of MBFC displacement depends on proper StC flattening, which supports the idea that these processes occur in a coordinated manner. Second, they identify the N pathway as playing an essential role in StC flattening. In addition to these new insights into follicular cell morphogenesis, my results also demonstrate that the N pathway acts during these morphogenetic events by controlling the dynamic of AJ disassembly and not cell identity.

StC differentiation and flattening

It has been previously shown that StC differentiation is a prerequisite for flattening (Xi et al., 2003). My data now show that differentiation is at least partly independent of flattening, since differentiation is still occurring in follicles with *fng* or *Dl Ser* mutant clones presenting impaired StC flattening. Surprisingly, in such follicles, supernumerary StC differentiate, which indicates that the number of cells fated to become StC is not determined until late stage 9 and that the identity of the centripetal cells and the MBFC are flexible. It is likely that in *fng* or *Dl Ser* mutant follicles, more cells differentiate and flatten to compensate for the abnormal flattening of the mutant StC, in order to maintain the integrity of the epithelium.

This indicates that the number of StC per follicle depends on their ability to flatten and on the size of the NC compartment, which is itself variable. The flexibility of the terminal cell population acquiring cell identity has previously been shown for border cell differentiation (Niewiadomska et al., 1999). Thus, although terminal cell differentiation is a prerequisite for morphogenesis, the two processes may be dependant on each other.

Forces controlling StC flattening and MBFC displacement

No cellular or molecular link has ever been established between border cell migration, StC flattening and MBFC displacement. It has been proposed that the displacement of the MBFC towards the oocyte starts within the posterior cells, which, by adopting a columnar shape, pull their anterior neighbours over the oocyte. As soon as these neighbouring cells contact the oocyte, they in turn adopt a columnar shape and pull on their anterior neighbouring cells (Horne-Badovinac and Bilder, 2005; Spradling, 1993). This process is helped by the growth of the oocyte. My results improve upon this model (Fig. 8), in particular by demonstrating that MBFC displacement depends on the capacity of the StC to flatten (1) and that this flattening depends on the pulling force generated by the posterior cells (2) and on forces generated by each StC, referred to as 'local forces' (3). These points are discussed individually below.

That MBFC displacement depends on the capacity of the StC to flatten is shown by three lines of evidence. First, MBFC displacement delays are observed in follicles in which *fng* or *Dl Ser* mutant clones encompass only, or mainly, the StC. Second, the

expressivity of this phenotype within a follicle depends on the proportion of the StC that are mutant. Third, MBFC displacement delays are always detected in *fng* or in *Dl Ser* mutant follicles that display abnormal dynamics in AJ disassembly in the StC.

Support for the suggestion that StC flattening depends on the pulling force created by the posterior cells comes first from previous observations of StC behaviour in *karst* mutant follicles and in *dicephalic* (*dic*) mutant follicles. In *karst* follicles, as the posterior cells do not adopt a columnar shape, it is proposed that the StC do not flatten because the pulling force is not generated (Zarnescu and Thomas, 1999). In *dic* follicles, the oocyte lies in the middle, with NC on either side surrounded by anterior terminal cells at the two extremities. Because of the position of the oocyte, the posterior end of the follicle is in the middle and the two extremities are both anterior ends (Gonzalez-Reyes et al., 1997; Gonzalez-Reyes and St Johnston, 1998; Lohs-Schardin, 1982). At stage 9, the cells that are in contact with the oocyte become columnar and presumably create the pulling force that acts on the StC located on both sides of the oocyte, to guide their flattening. Second, the shape of the StC after they have flattened in WT follicles is more elongated along the A/P axis than along the D/V axis. This reveals that the direction of the elongation of the cells is not random, but is instead most likely a consequence of the localization of the pulling force.

The final point is that the capacity of the StC to flatten depends on local forces. Indeed, the shape of the StC and their coordinated flattening are dependent on the pattern of AJ disassembly at stage 9. This pattern, with the three-cell junctions disassembling first, followed

by the AJ becoming oriented perpendicularly, rather than parallel, to the A/P axis of the follicle (Fig. 8), exerts constraints on the cells and prevents them from flattening in a uniform and non-directional manner. If this cell-autonomous activity is impaired, the StC do not flatten properly and the flattening that does occur is no longer coordinated around the follicle, as observed in *fng* or *Dl Ser* mutant follicles. Thus, StC flattening depends, in part, on the cell-autonomous ability of each StC to control AJ disassembly. This control can be a response of the cells that sense and integrate the mechanical strain exerted by the pulling force, or can occur independently of the action of the pulling force. Finally, as any force involves the regulation of the actin network, the observation that two proteins linking to the actin cytoskeleton (E Cad and Myosin II) are required for proper StC flattening, supports the existence of local forces.

In conclusion, the flattening of the StC is driven by the pulling force and local forces, which together facilitate AJ disassembly in a polarized manner. As a result, both forces coordinate the rate of StC flattening and orient its direction. In parallel, these two forces, with the growth of the oocyte, define the rate of MBFC displacement. Thus, MBFC displacement and StC flattening are morphogenetic processes that are linked at a cellular level.

The Notch pathway controls the dynamics of AJ remodelling

In contrast to the well-studied role of *N* in cell identity determination, the data presented here provides, to my knowledge, the first example in which the N pathway is described as playing a

role in AJ disassembly and raises the question of whether this role can be extended to other biological contexts. Previous analyses have reported a requirement of *N* during late oogenesis using the N^{ts1} allele (Dobens et al., 2005; Gonzalez-Reyes and St Johnston, 1998; Keller Larkin et al., 1999; Zhao et al., 2000), but none of them have established its precise function. Here, I demonstrate that a *fng*-dependent N activity is required in the StC and in the most anterior MBFC at stage 9 of oogenesis for StC flattening and to control the timing of MBFC displacement. Moreover, the higher accumulation of N at disassembling junctions relative to intact junctions in the StC, at the exact moment that disassembly is required, supports the fact that the role for N in StC flattening is directly related to this specific and strong accumulation. Finally, the pattern of expression of reporters of N activation and the defects observed when *H* is overexpressed in the StC, indicate that N acts in these processes through the canonical pathway. However, as I failed to detect any alterations in cell identity, it is possible that the differentiation defects observed with the N^{ts1} allele are due to its earlier requirement in the arrest of follicular cell mitotic divisions at stage 6 (Deng et al., 2001). Alternatively, the differentiation of some of the terminal populations might be affected by clones encompassing more, or different, follicular cells than the ones I have focused on in this work. Extensive clonal analyses of *Dl Ser* mutant clones should help resolve this issue.

The activation of the local forces or the modifications of the expression and/or localisation of adhesion molecules could either be responses to the pulling force or could occur independently of it. One of the major keys to understanding the role of N in AJ disassembly is

thus to determine whether N acts on the reception and/or the integration of the pulling force, or directly on the generation of local forces and on the control of the expression and/or localisation of adhesion molecules. As for the possibility that N controls local forces, it is striking that Zip accumulation is delayed at the AJ that should have been disassembled in *Dl Ser* mutant clones. Indeed, recent studies have shown the importance of the accumulation of Zip and Sqh at disassembling junctions for cell intercalation during germ-band elongation in the *Drosophila* embryo (Bertet et al., 2004). During this process, AJ remodelling occurs with a very specific ordered pattern and the localisation of Myosin II mirrors this pattern. The authors also show that disrupting Myosin II activity genetically or chemically leads to an absence of indicators of AJ remodelling and defects in cell intercalation. In light of these observations, my data suggest a model for AJ disassembly during StC flattening, in which the N pathway acts on the generation of local forces by controlling a polarized accumulation of Zip, which in turn remodel AJ between the StC (Fig. 8). How N controls the localisation of Myosin II and how Myosin II remodels AJ locally remains to be determined. Finally, the persistence of NCad expression after stage 7 in *shg* mutant clones supports the hypothesis that the control of the expression and/or the localisation of adhesion molecules is through multiple routes.

Materials and Methods

Drosophila Stocks and Crosses

fng^{13}, *Dl*^{rev10}, *Ser*$^{rev2-11}$, *Ser*^{RX106}, *shg*^{R69} are null alleles (de Celis et al., 1993; Godt and Tepass, 1998; Heitzler and Simpson, 1991; Irvine and Wieschaus, 1994; Sun and Artavanis-Tsakonas, 1996) and *sqh*^{1} is an hypomorph allele (Karess et al., 1991). CantonS was used as wild-type, and reporter lines used were *sqh*^{AX3}; P(*w*$^{+}$, SqhGFP)40 (Royou et al., 2002), *MA33* (Gonzalez-Reyes and St Johnston, 1998), *dpp-lacZ* (Jiang and Struhl, 1995), *Dad-lacZ* (Kai and Spradling, 2003), *Dl-lacZ* (Grossniklaus et al., 1989), *E(spl)mβ7-lacZ* (an enhancer-trap in the *E(spl)mβ7* gene, gift of S. Bray, University of Cambridge, Cambridge, UK) and *E(spl)mβ-CD2* (Cooper and Bray, 1999). *sqh*^{1}, *shg*^{R69}, *fng*^{13}, *Dl*^{rev10}, *Ser*$^{rev2-11}$, and *Dl*^{rev10}Ser^{RX106} clones were generated by Flipase-mediated mitotic recombination on FRT101, FRT42D, FRT80-3 or FRT82B chromosomes, and marked using *π-Myc* or *GFP* transgenes (Xu and Rubin, 1993). Ectopic expression of activated-Notch was performed by generating Flip-out Gal4 clones in animals carrying UAS-ΔN34a (Doherty et al., 1996) and *AyGal4 UASGFP* (Ito et al., 1997) transgenes. Flipase expression was induced by heat shocking two-day old females at 38°C for 1 hour to generate mutant clones and at 32.5°C for 30 minutes to generate Flip-out clones. Ectopic expression of *Hairless* (Johannes and Preiss, 2002) was performed by heat shocking, 6 hours before dissecting, three to five-day old females at 36.5°C for 1 hour.

Follicle Staining

Immunofluorescent staining of follicles was carried out as described previously (Grammont and Irvine, 2001) using goat anti-ß-galactosidase (1:1000, Biogenesis), rabbit anti-Myc (1:100, Santa Cruz), mouse anti-GFP (1:500, Sigma-Aldrich), rabbit anti-Zipper (1/1000, (Jordan and Karess, 1997)) mouse anti-Eya (1:500, Developmental Studies Hybridoma Bank (DSHB)), mouse anti-αTub (1:1000, clone DM1A, Sigma-Aldrich), rat anti-ECad (1:200, DSHB), mouse anti-Arm (1/50, DSHB) and rat anti-NCad (1:20, DSHB) with the following modification: ovaries from females were dissected directly into fixative, five to seven days after Flipase induction (36 hours for *sqh* mutant clones).

Description of the markers used

Follicles were staged according to King (1970) and Spradling (1993).

MA33 is expressed only in the stretched cells from stage 9 onwards (Gonzalez-Reyes and St Johnston, 1998; Grammont and Irvine, 2002; Silver et al., 2005; Xi et al., 2003). *Dpp-lacZ* is also specifically expressed in the stretched cells at stage 9, as it turns on in some centripetal cells only at stage 10B (Dobens et al., 2000; Xi et al., 2003). Eya expression is specific, at stage 9, to border and stretched cell fates (Bai and Montell, 2002). In WT stage 9 follicles, the expression of these markers occurs progressively from the anterior part of the follicle and progresses posteriorly row by row as a wave. Accordingly, a gradient of expression for all these markers is

detected in the anterior part of a stage 9 follicle, with the strongest expression in the already flattened StC, a weaker expression in the flattening StC and the weakest expression in the cells that are about to undergo flattening. Since Eya is expressed in both border and stretched cells at stage 9, any conclusions drawn from an Eya staining were always confirmed with MA33, *dpp-lacZ* or *Dad-lacZ* to avoid ambiguity concerning the fate of the cells. *Dad* was used as a stretched cell fate marker, since its expression pattern is similar to that of *dpp-lacZ* during stage 9. Surface areas of StC were determined with the LSM510Meta software. Follicles were flattened under a cover slip, such that the StC in immediate contact with either the cover slip or the slide (i.e. those on the top or the bottom of the follicle) could be viewed within a single focal plane. Only these StC were used for surface area calculations in order to avoid inaccuracies caused by the natural curvature of the follicle, which is not taken into account.

Imaging

Confocal images were obtained using a Zeiss LSM510Meta microscope with 40x/1.3 Plan-NeoFluar and 63x/1.4 Plan-Apochromat objectives. All imaging was done at RT. Figures were processed using the LSM510Meta software and Photoshop 7 (Adobe Systems) and Freehand 10 (macromedia). In all panels, unless otherwise stated, the focus is on the upper plane and a projection (z stack) of all the z-sections in which the stretched cells are visible, is presented.

Online Supplemental Material

Supplemental data S1: “Arm expression pattern mirrors AJ remodeling” describes the expression of Arm in WT follicles and in *Dl Ser* mutant follicles.

Supplemental data S2: “AJ remodeling in *fng* mutant follicles is delayed, but not blocked” describes the expression of ECad in stage 10A *fng* mutant follicle.

Supplemental data S3: “StC flattening and AJ remodeling required transcriptional activity of the N pathway” describes the expression of *Dl-lacZ*, *E(spl)mβ7-lacZ* and *E(spl)mβ-CD2* reporters in stage 9 follicles, the delay in AJ remodelling observed in stage 9 follicles overexpressing *H* and in stage 9 follicles overexpressing Nact.

Supplemental data S4: “*shg* controls the down-regulation of NCad” describes the expression of NCad in *shg* mutant clones at stage 7 and 8.

Acknowledgements

I thank R. Karess, L. Dobens, D. Godt, A. Preiss, F. Schweisguth, K. Irvine, the DSHB and the Bloomington Stock Center for antibodies and *Drosophila* stocks and R. Karess, D. Godt, K. Irvine, F. Schweisguth, C. Vachias, O. Bardot, J.L. Couderc and P. Das for helpful remarks and comments on the manuscript.

This research was supported by the Institut National de la Santé et de la Recherche Médicale.

Abbreviations list

AJ : Adherens junctions

A/P: Antero-posterior

MBFC: Main body follicular cells

NC: Nurse cells

StC: Stretched cells

WT: Wild type

References

Bai, J., and D. Montell. 2002. Eyes absent, a key repressor of polar cell fate during Drosophila oogenesis. *Development*. 129:5377-88.

Beccari, S., L. Teixeira, and P. Rorth. 2002. The JAK/STAT pathway is required for border cell migration during Drosophila oogenesis. *Mech Dev*. 111:115-23.

Bertet, C., L. Sulak, and T. Lecuit. 2004. Myosin-dependent junction remodelling controls planar cell intercalation and axis elongation. *Nature*. 429:667-71.

Cooper, M.T., and S.J. Bray. 1999. Frizzled regulation of Notch signalling polarizes cell fate in the Drosophila eye. *Nature*. 397:526-30.

de Celis, J.F., R. Barrio, A. del Arco, and A. Garcia-Bellido. 1993. Genetic and molecular characterization of a Notch mutation in its Delta- and Serrate-binding domain in Drosophila. *Proc Natl Acad Sci U S A*. 90:4037-41.

Deng, W.M., C. Althauser, and H. Ruohola-Baker. 2001. Notch-Delta signaling induces a transition from mitotic cell cycle to endocycle in Drosophila follicle cells. *Development*. 128:4737-46.

Dobens, L., A. Jaeger, J.S. Peterson, and L.A. Raftery. 2005. Bunched sets a boundary for Notch signaling to pattern anterior eggshell structures during Drosophila oogenesis. *Dev Biol*. 287:425-37.

Dobens, L.L., J.S. Peterson, J. Treisman, and L.A. Raftery. 2000. Drosophila bunched integrates opposing DPP and EGF signals to set the operculum boundary. *Development*. 127:745-54.

Dobens, L.L., and L.A. Raftery. 2000. Integration of epithelial patterning and morphogenesis in Drosophila ovarian follicle cells. *Dev Dyn*. 218:80-93.

Doherty, D., G. Feger, S. Younger-Shepherd, L.Y. Jan, and Y.N. Jan. 1996. Delta is a ventral to dorsal signal complementary to Serrate, another Notch ligand, in Drosophila wing formation. *Genes Dev*. 10:421-34.

Godt, D., and U. Tepass. 1998. Drosophila oocyte localization is mediated by differential cadherin- based adhesion. *Nature*. 395:387-91.

Gonzalez-Reyes, A., H. Elliott, and D. St Johnston. 1997. Oocyte determination and the origin of polarity in Drosophila: the role of the spindle genes. *Development*. 124:4927-37.

Gonzalez-Reyes, A., H. Elliott, and R.D. St. Johnston. 1995. Polarization of both major body axes in Drosophila by gurken-torpedo signalling. *Nature*. 375:654--658.

Gonzalez-Reyes, A., and D. St Johnston. 1998. Patterning of the follicle cell epithelium along the anterior-posterior axis during Drosophila oogenesis. *Development*. 125:2837-46.

Grammont, M., and K.D. Irvine. 2001. fringe and Notch specify polar cell fate during Drosophila oogenesis. *Development*. 128:2243-53.

Grammont, M., and K.D. Irvine. 2002. Organizer activity of the polar cells during Drosophila oogenesis. *Development*. 129:5131-40.

Grossniklaus, U., H.J. Bellen, C. Wilson, and W.J. Gehring. 1989. P-element-mediated enhancer detection applied to the study of oogenesis in Drosophila. *Development*. 107:189--200.

Heitzler, P., and P. Simpson. 1991. The choice of cell fate in the epidermis of Drosophila. *Cell*. 64:1083--1092.

Horne-Badovinac, S., and D. Bilder. 2005. Mass transit: epithelial morphogenesis in the Drosophila egg chamber. *Dev Dyn*. 232:559-74.

Irvine, K.D., and E. Wieschaus. 1994. fringe, a Boundary-specific signaling molecule, mediates interactions between dorsal and ventral cells during Drosophila wing development. *Cell*. 79:595-606.

Ito, K., H. Sass, J. Urban, A. Hofbauer, and S. Schneuwly. 1997. GAL4-responsive UAS-tau as a tool for studying the anatomy and development of the Drosophila central nervous system. *Cell Tissue Res*. 290:1-10.

Jiang, J., and G. Struhl. 1995. Protein kinase A and hedgehog signaling in Drosophila limb development. *Cell*. 80:563-72.

Johannes, B., and A. Preiss. 2002. Wing vein formation in Drosophila melanogaster: hairless is involved in the cross-talk between Notch and EGF signaling pathways. *Mech Dev*. 115:3-14.

Jordan, P., and R. Karess. 1997. Myosin light chain-activating phosphorylation sites are required for oogenesis in Drosophila. *J Cell Biol*. 139:1805-19.

Kai, T., and A. Spradling. 2003. An empty Drosophila stem cell niche reactivates the proliferation of ectopic cells. *Proc Natl Acad Sci U S A*. 100:4633-8.

Karess, R.E., X.J. Chang, K.A. Edwards, S. Kulkarni, I. Aguilera, and D.P. Kiehart. 1991. The regulatory light chain of nonmuscle myosin is encoded by spaghetti-squash, a gene required for cytokinesis in Drosophila. *Cell*. 65:1177-89.

Keller Larkin, M., W.M. Deng, K. Holder, M. Tworoger, N.J. Clegg, and H. Ruohola-Baker. 1999. Role of Notch pathway in terminal follicle cell differentiation during Drosophila oogenesis. *Dev Genes Evol*. 209:301-11.

King, R.C. 1970. Ovarian Development in Drosophila melanogaster. Academic Press, New York. x + 227pp pp.

Lohs-Schardin, M. 1982. Dicephalic - a Drosophila mutant affecting polarity in follicle organization and embryonic patterning. *Roux Arch. dev. Biol*. 191:28--36.

Lopez-Schier, H., and D. St Johnston. 2001. Delta signaling from the germ line controls the proliferation and differentiation of the somatic follicle cells during Drosophila oogenesis. *Genes Dev*. 15:1393-405.

Niewiadomska, P., D. Godt, and U. Tepass. 1999. DE-Cadherin is required for intercellular motility during Drosophila oogenesis. *J Cell Biol*. 144:533-47.

Roth, S., F.S. Neuman-Silberberg, G. Barcelo, and T. Schupbach. 1995. cornichon and the EGF receptor signaling process are necessary for both anterior-posterior and dorsal-ventral pattern formation in Drosophila. *Cell*. 81:967--978.

Royou, A., W. Sullivan, and R. Karess. 2002. Cortical recruitment of nonmuscle myosin II in early syncytial Drosophila embryos: its role in nuclear axial expansion and its regulation by Cdc2 activity. *J Cell Biol*. 158:127-37.

Silver, D.L., E.R. Geisbrecht, and D.J. Montell. 2005. Requirement for JAK/STAT signaling throughout border cell migration in Drosophila. *Development*. 132:3483-92.

Silver, D.L., and D.J. Montell. 2001. Paracrine signaling through the JAK/STAT pathway activates invasive behavior of ovarian epithelial cells in Drosophila. *Cell*. 107:831-41.

Spradling, A.C. 1993. Development Genetics of Oogenesis. *In* The Development of Drosophila melanogaster. M. Bate and A. Martinez-Arias, editors. Cold Spring Harbor Laboratory Press, Cold Spring Harbor, N.Y. 1-70.

Sun, X., and S. Artavanis-Tsakonas. 1996. The intracellular deletions of Delta and Serrate define dominant negative forms of the Drosophila Notch ligands. *Development*. 122:2465-74.

Torres, I.L., H. Lopez-Schier, and D. St Johnston. 2003. A Notch/Delta-dependent relay mechanism establishes anterior-posterior polarity in Drosophila. *Dev Cell*. 5:547-58.

Xi, R., J.R. McGregor, and D.A. Harrison. 2003. A gradient of JAK pathway activity patterns the anterior-posterior axis of the follicular epithelium. *Dev Cell*. 4:167-77.

Xu, T., and G.M. Rubin. 1993. Analysis of genetic mosaics in developing and adult Drosophila tissues. *Development*. 117:1223-37.

Zarnescu, D.C., and G.H. Thomas. 1999. Apical spectrin is essential for epithelial morphogenesis but not apicobasal polarity in Drosophila. *J Cell Biol*. 146:1075-86.

Zhao, D., D. Clyde, and M. Bownes. 2000. Expression of fringe is down regulated by Gurken/Epidermal Growth Factor Receptor signalling and is required for the morphogenesis of ovarian follicle cells. *J Cell Sci*. 113 Pt 21:3781-94.

Figure 1

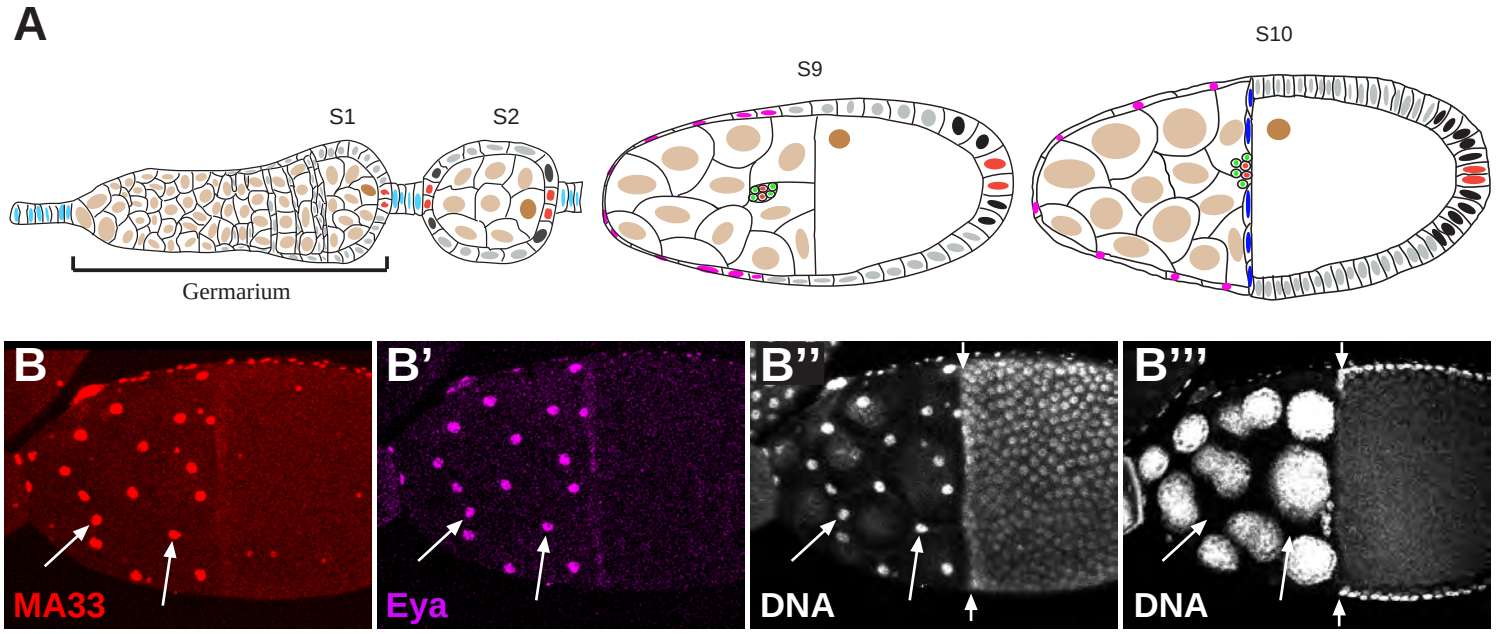

Figures legends

Fig. 1. Schematic of follicular cell populations.

In all figures, anterior is to the left. (A) Schematic of a wild-type ovariole. The arrangement and identities of the different cells - oocyte (nucleus coloured in brown), NC (tan), follicular cells (S1) or MBFC (from S2 to S14) (gray), polar cells (red), stalk cells (light blue), terminal cells (dark gray), border cells (green), StC (pink), centripetal cells (dark blue) and posterior cells (black) - are shown in the germarium and in stage 2 (S2), 9 (S9) and 10 (S10) follicles. (B) StC nuclei of the stage 10 WT follicle (long arrows). B''' is focused on the medial plane. Small arrows indicate the border between the oocyte and the NC.

Figure 2

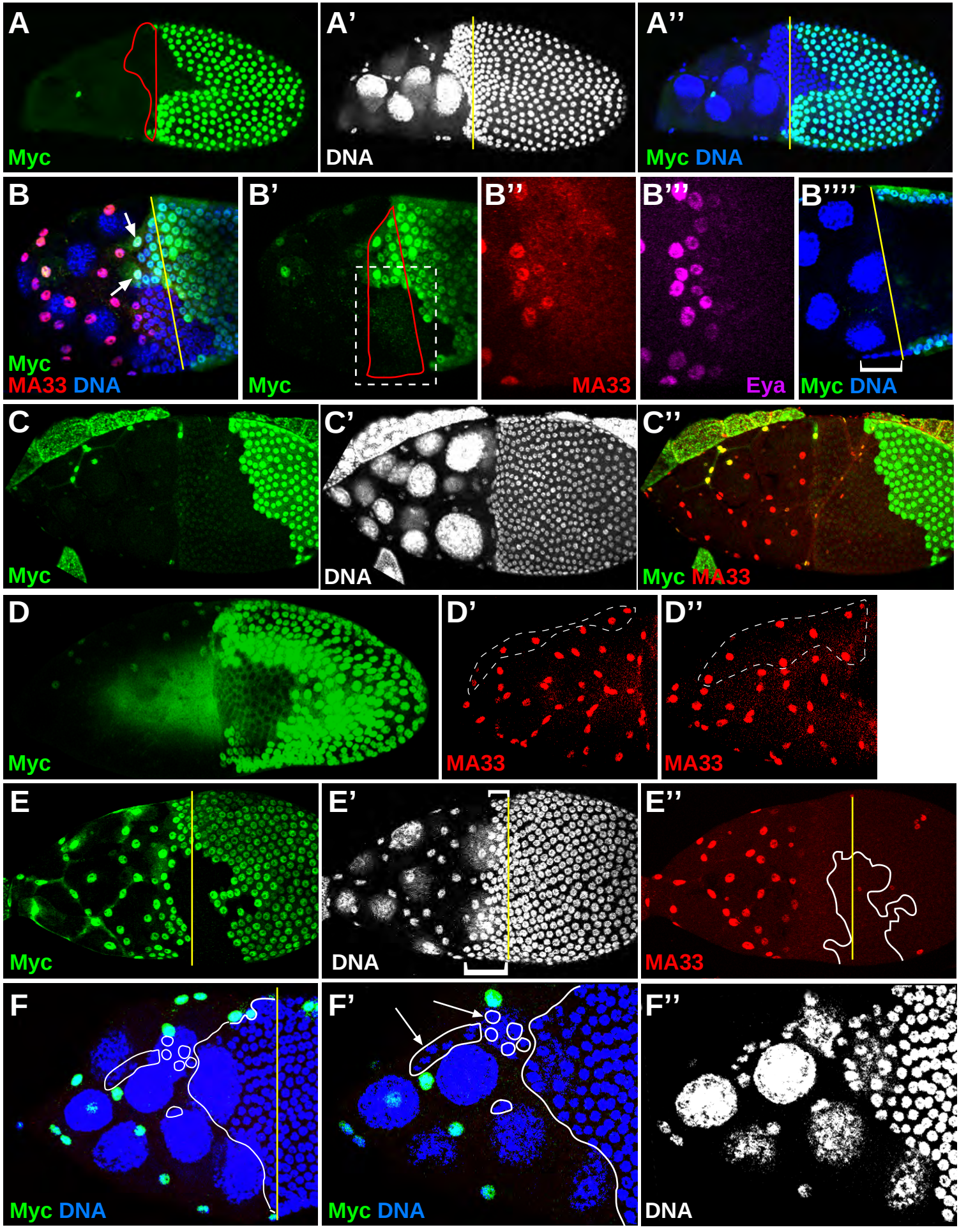

Fig. 2. *fng* is required in the StC and in the anterior MBFC to control StC number and the timing of the MBFC displacement.

Follicles of stage 10A (A, B, E, F) or stage 10B (C, D) with *fng*^{13} clones marked by the absence of Myc. The yellow line marks the border between the NC and the oocyte. (A) The cluster of cells (outlined in red in A) overlying the NC presents a density of nuclei similar to the density of MBFC nuclei. (B) A cluster of cells (outlined in red in B') with a high density of nuclei overlies the NC. Some cells of the clusters are WT (arrows). B'' and B''' are magnified views on the boxed area in B'. The anterior cells of such clusters express a StC fate (B'', B'''). B'''' is focused on the medial plane showing some MBFC overlying a NC (bracket). (C) A follicle with a clone encompassing some StC and MBFC. No cluster of cells with a high density overlies the NC. (D) D is a composite view of all the z-sections throughout the follicle whereas D' and D'' are focused on the upper and lower planes of the follicle respectively. All the cells overlying the NC have a StC fate and are 43 and 36 in number in the two focal planes shown (D' and D''). The few WT StC are outlined with a dashed line. (E) A follicle with a clone encompassing only some MBFC (outline in white in E''). More MBFC overlie the NC in the mutant region (larger bracket) than in the WT region (smaller bracket). (F) A follicle with a large *fng* clone encompassing most of the MBFC and a few StC. An abnormally high number of cells is visible over the NC. F' and F'' are magnified views of the anterior part with a focus on the StC. The mutant cells are outlined in white. MBFC posterior to WT StC are less delayed than MBFC posterior to unflattened mutant StC (arrows).

Figure 3

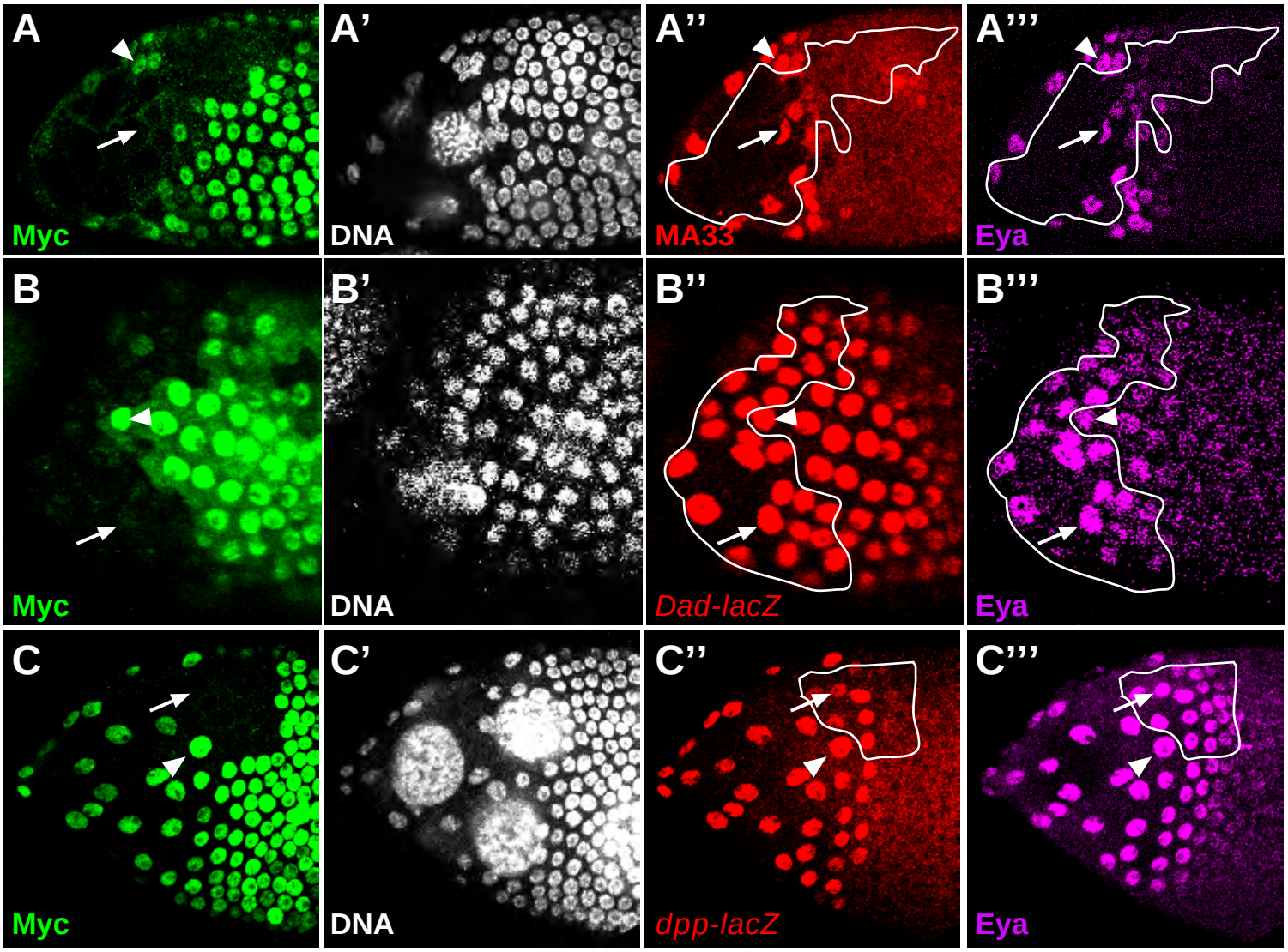

Fig. 3. *fng* is not required for StC differentiation. Stage 9 follicles with *fng*^{13} clones (outlined in white) spread over only on one side of the follicle and marked by the absence of Myc. Expressions of MA33 (A), *Dad-lacZ* (B), *dpp-lacZ* (C) and Eya (A, B, C) are not affected in mutant cells (arrows) in comparison to WT cells (arrowheads) located at the same A/P position.

Figure 4

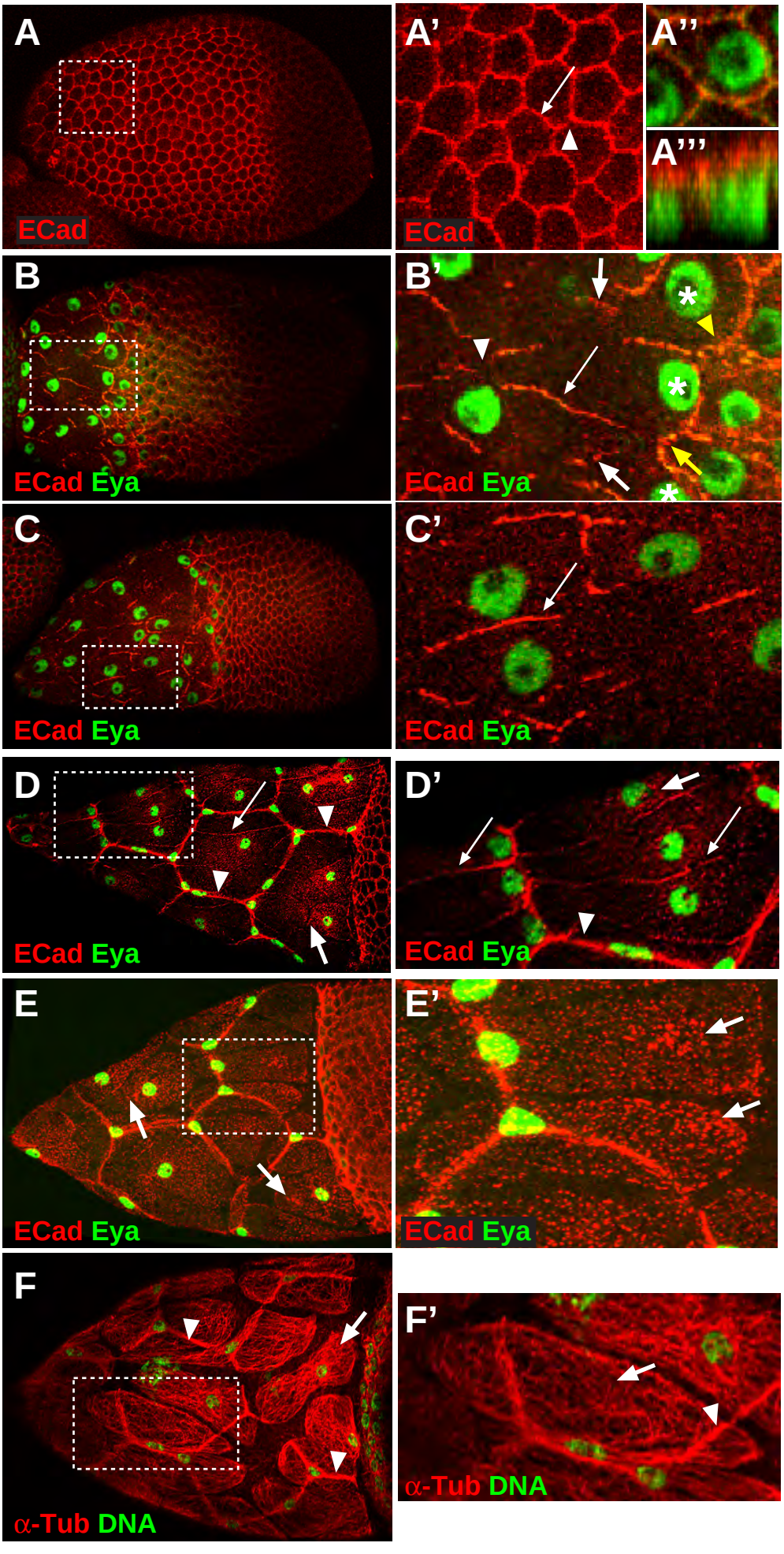

Fig. 4. Adherens junction remodelling in WT follicles. A'-F' are magnified views of the boxed areas in A-F. (A) An early stage 9 follicle showing the hexagonally shaped follicular cells that make contact through two-cell (arrow) or three-cell junctions (arrowhead). A''' is a z-section of the follicular cell shown in A''. AJ are localised apically (A'', A'''). (B) A mid stage 9 follicle. The asterisks indicate the StC undergoing flattening. ECad is not detected at the three-cell junction between flattened and flattening cells (white arrowhead), but is visible between flattening and unflattened cells (yellow arrowhead). Spots of ECad are present at the perpendicularly-oriented junctions between flattened and flattening cells (short white arrow). ECad is strongly detected at the perpendicularly-oriented junctions between flattening and unflattened (yellow arrow) and at the junctions oriented parallel to the A/P axis (long white arrow). (C) A late stage 9 follicle with most of the AJ parallel to the A/P axis stained (arrow). (D) A stage 10A follicle, where ECad is detected in the part of the StC that is squeezed into the interstitial gaps between NC (arrowheads). The AJ parallel to the A/P axis are faintly detectable (long arrows), but ECad increases in the part of the StC overlying the NC (short arrows). (E) A stage 10B follicle, where the AJ parallel to the A/P axis are no longer visible. ECad is accumulated in the part of the StC that overlies the NC (arrows). (F) A stage 10B follicle with a Tubulin network present in the cytoplasm of the StC that is squeezed into the gaps between NC (arrowheads) and in the cytoplasm overlying the NC (arrows).

Figure 5

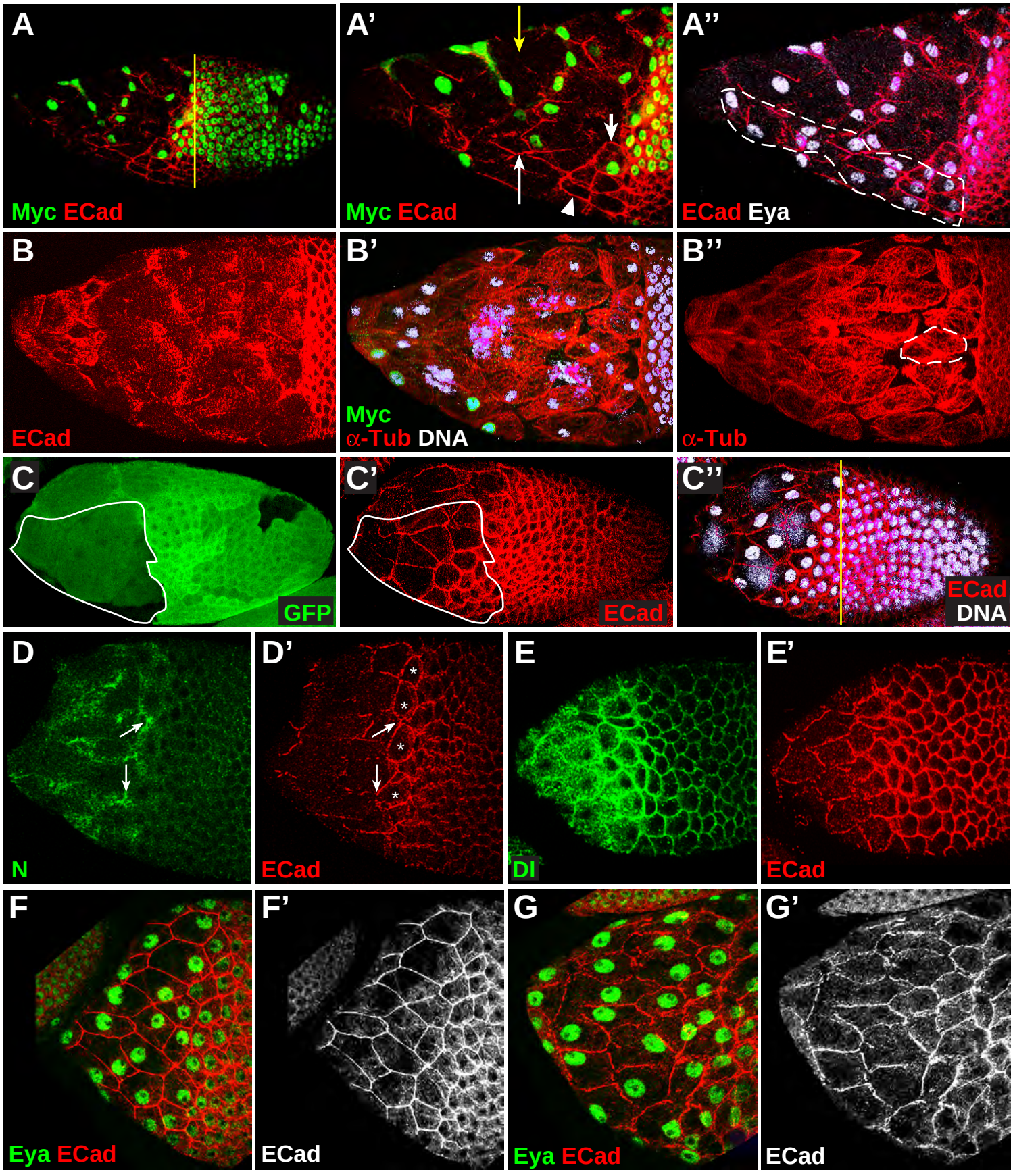

Fig. 5. The N pathway is required for the dynamics of AJ remodelling. The yellow line marks the border between the NC and the oocyte. (A, B) Follicles with *fng*^{13} clones marked by the absence of Myc. (A) A late stage 9 follicle with a *fng* clone encompassing some StC and MBFC. A' and A'' are magnified views of the anterior part of the follicle shown in A. The three-cell junctions are disassembled in the WT region (yellow arrow) but are still present in the mutant region (long arrow). More posteriorly, ECad is still present all around the edges of the cells in the mutant region (arrowhead). A WT cell also displays this pattern (short arrow). More StC differentiated in the mutant region (outlined in white) and MBFC displacement is delayed. (B) A stage 10B follicle with a large *fng*^{13} clone. An abnormally high number of StC is observed and the surface area of one of them is outlined. (C) A stage 10A follicle with a *Dl*^{rev10} *Ser*^{RX106} clone, marked by the absence of GFP, encompassing some StC and MBFC (outline in white). GFP expression is also visible in the germline cells. Also apparent are delays in MBFC displacement and AJ remodelling. (D, E) WT follicles. The flattening StC are marked with an asterisk. N is specifically accumulated at the disassembling three-cell junctions (arrows). (F, G) Follicles overexpressing *H*. (F) No AJ disassembly are detected in an early-mid stage 9 follicle. (G) Some three cell-types junctions are disassembling in some StC in a mid-late stage 9 follicle.

Figure 6

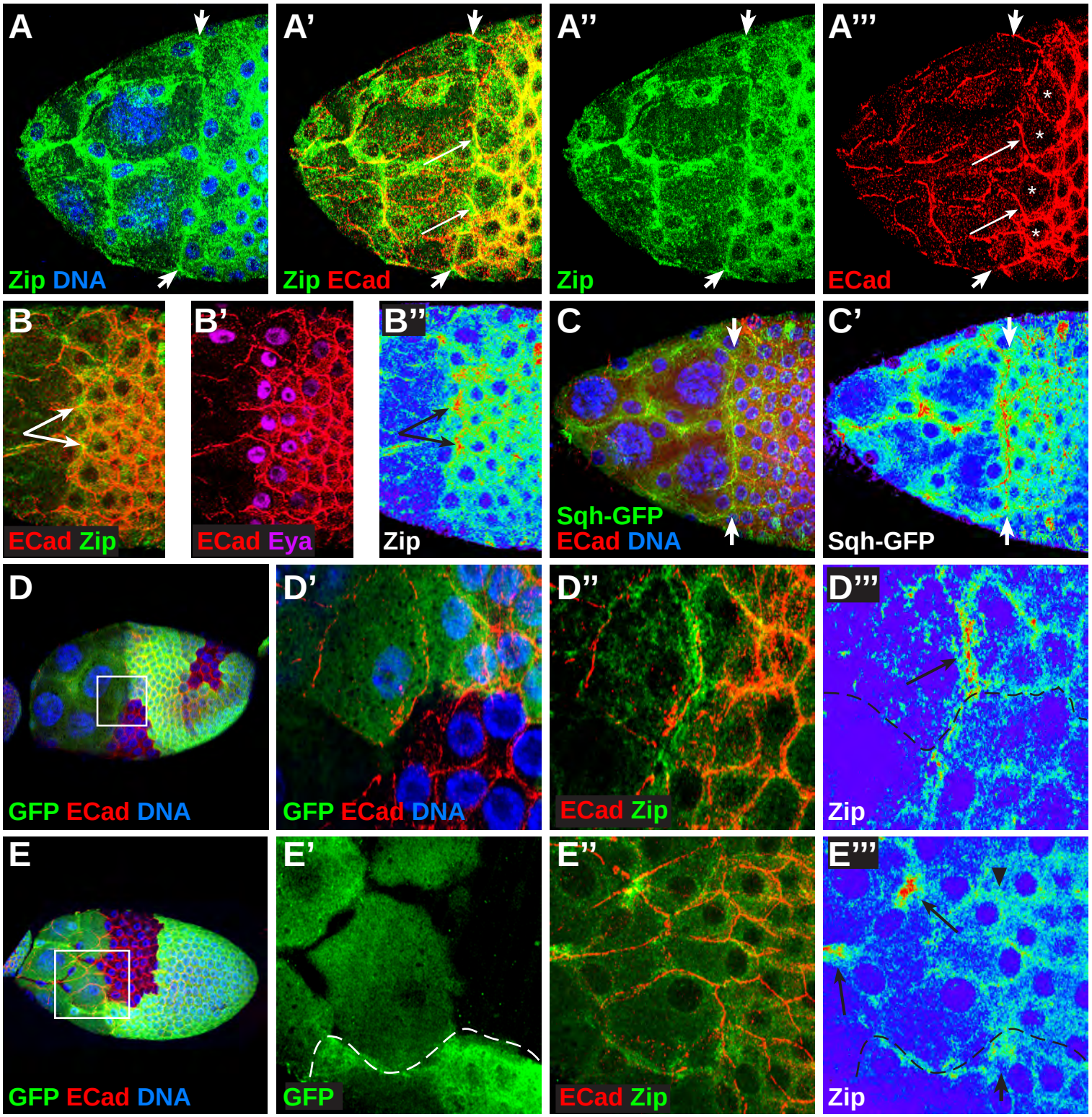

Fig. 6. The N pathway controls the localisation of Myosin II. The use of a colour gradient allows the visualization of differences in intensities of accumulation from none (black) to strongest (red). (A–C) Mid stage 9 WT follicles. (A) A line of Zip expression (flanked by short arrows) perpendicular to the A/P axis is detected at the boundary between flattened and flattening StC (marked with an asterisk). This line comprises some of the junctions perpendicular to the A/P axis (long arrow). (B) Zip is accumulating more strongly at the three-cell junctions between flattening and unflattened StC (arrows). (C) Sqh-GFP expression. A line of Sqh-GFP expression (flanked by arrows) perpendicular to the A/P axis is detected at the boundary between flattened and flattening StC. (D, E) Follicles with Dl^{rev10} Ser^{RX106} clones marked by the absence of GFP. MBFC displacement is delayed in the mutant region (D, E). D'-D''' and E'-E''' are magnified views of the boxed areas in D and in E. (D) Zip is strongly accumulated along a line perpendicular to the A/P axis in the WT region (arrow), which stops at the boundary of the mutant clone (outlined in black). (E) Zip is strongly accumulated at disassembling three-cell junctions in the WT region (short arrow). No accumulation of Zip is detected in the mutant region at the same A/P position (arrowhead), but an accumulation is detected more anteriorly (long arrows). The boundary between WT and mutant regions is outlined in white (E') or in black (E''').

Figure 7

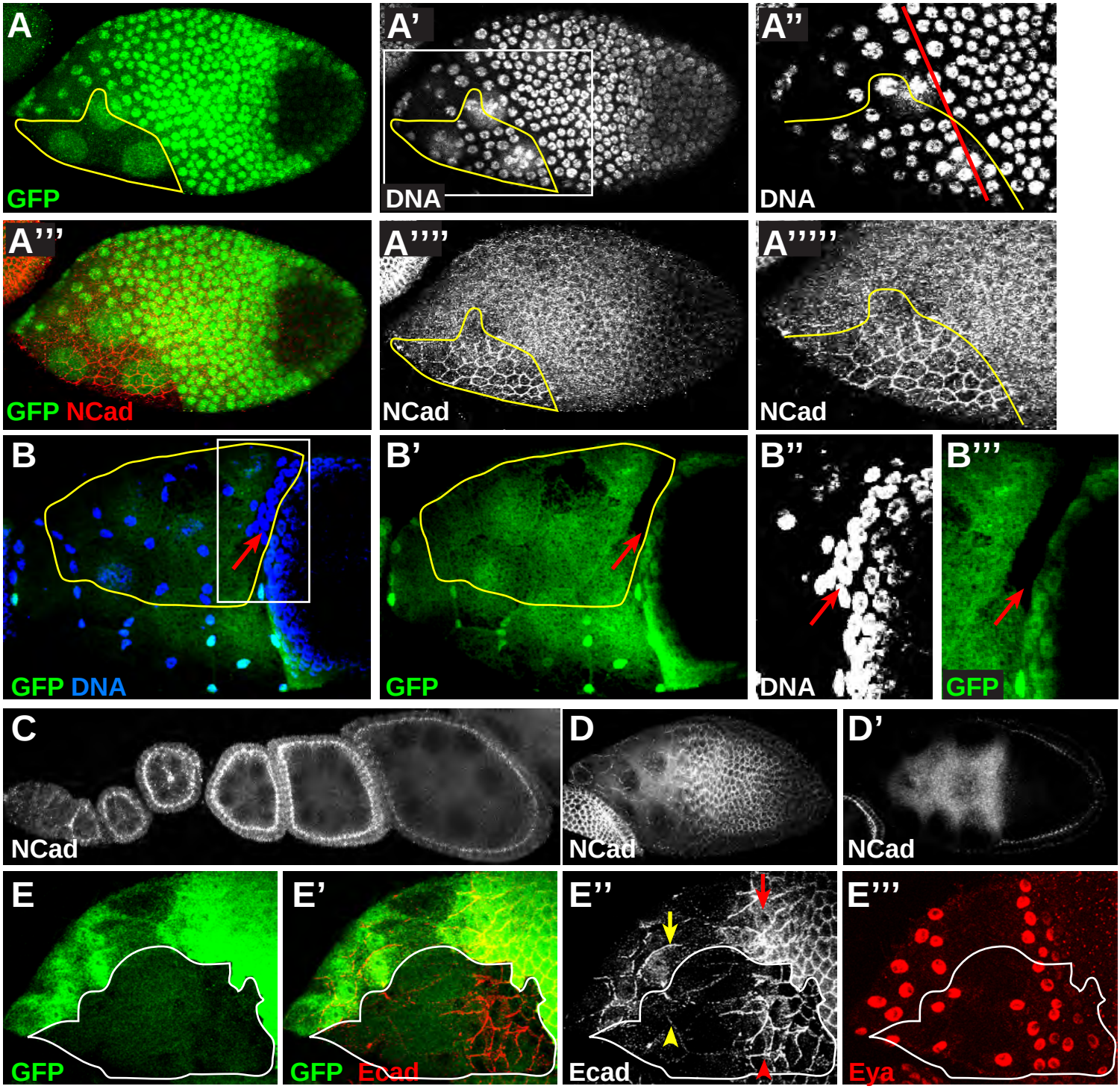

Fig. 7. ECad and Myosin II are required for proper StC flattening, the timing of MBFC displacement and AJ remodelling. All clones are outlined in yellow in A and B and in white in E. In C and D', the focus is on the medial plane. (A, B) Follicles with *shg*^{R69} clones, marked by the absence of GFP, encompass some StC and some MBFC. (A) A mid stage 9 follicle with a higher density of StC in the mutant region. A higher expression of NCad is observed in the mutant clone. A'' and A'''' are magnified views on the boxed area in A'. The red line marks the border between flattening and unflattened StC. (B) A stage 10A follicle with delayed MBFC displacement (arrow) in a mutant region. B'' and B''' are magnified views on the boxed area in B. (C, D) WT ovariole (C) and stage 9 follicle (D) stained for NCad. (E) Stage 9 follicle with *sqh*^{1} clone, marked by the absence of GFP, encompassing some StC and some MBFC. The elongation of the cells (red arrows in mutant and red arrowheads in WT) is no longer oriented in the mutant region and the AJ parallel to the A/P axis between mutant cells that have already flattened are no longer visible (yellow arrows - compared to yellow arrowheads in WT).

Figure 8

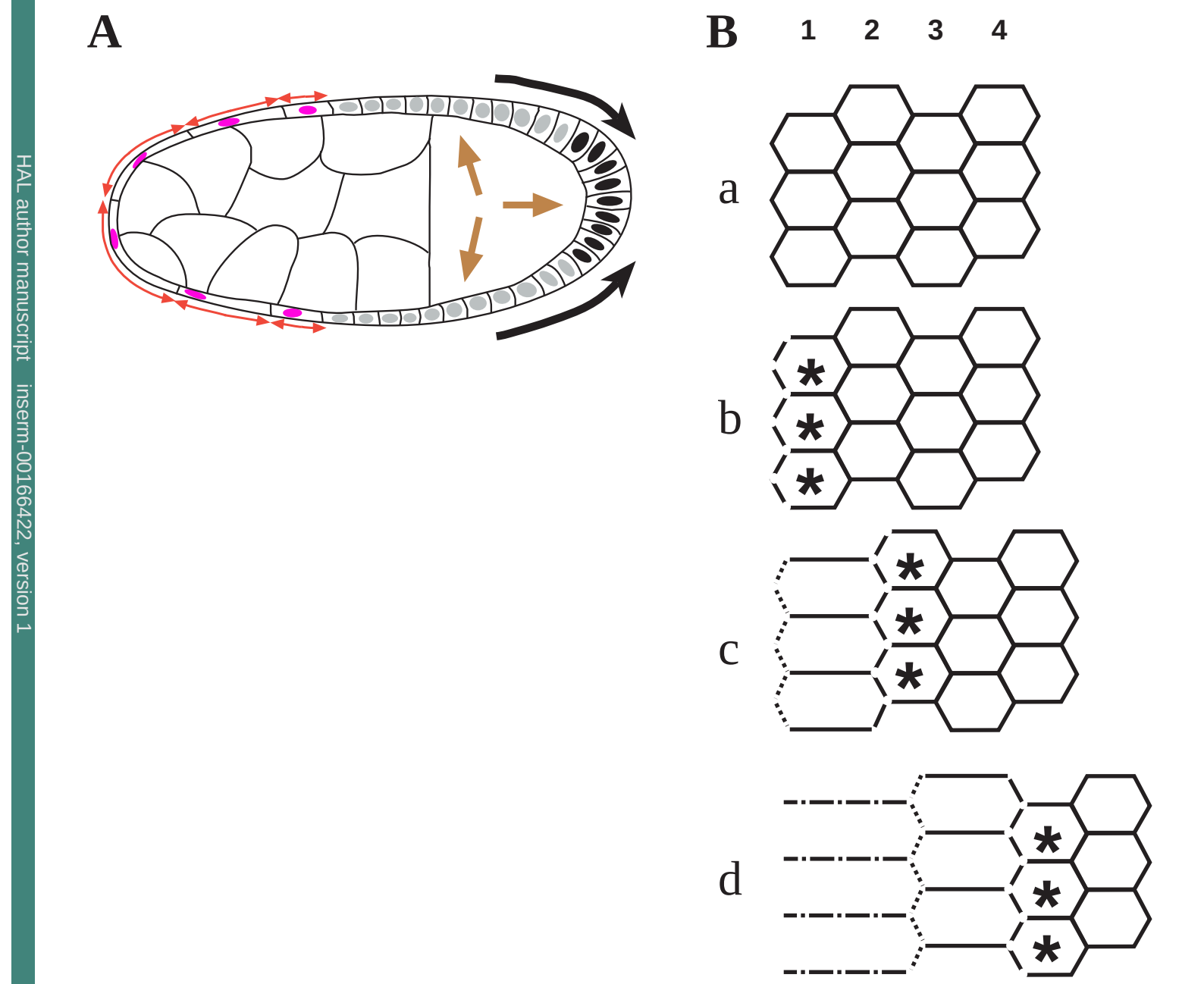

Fig. 8. Model of the morphogenesis of the follicular cells. (A) Schematic of a stage 9 follicle. The different populations of somatic cells - StC (nuclei colored in pink), MBFC (gray) and posterior cells (black) - are shown, as well as the forces involved in StC flattening and MBFC displacement - pulling force (black arrows), oocyte growth (brown arrows) and local forces (red double arrows). (B) Schematic of AJ disassembly in StC during stage 9. The AJ of four rows of three StC are represented at various stages of flattening. The asterisks mark the flattening StC. (a) Before flattening, the cells have a hexagonal shape. (b) In row 1, the anterior three-cell junctions are disassembling. (c) In row 1, the anterior two-cell junctions perpendicular to the A/P axis are disassembling as well as the three-cell junctions between rows 1 and 2, allowing the elongation of the cells along the A/P axis. The junctions parallel to the A/P axis of row 1 are intact. (d) In row 1, the cells are fully flattened. Their junctions parallel to the A/P are still present. The two-cell junctions perpendicular to the A/P axis between rows 1 and 2, are disassembling and the three-cell junctions between row 2 and 3 are disassembled.